Simulation and analysis of spacecraft charging using SPIS-GEO and NASCAP-GEO

B. Theillaumas, M. Sévoz, B. Andersson, T. Nilsson, J.C. Matéo-Vélez, P. Sarrailh, B. Thiébault, Ruard Jeanty, D. Rodgers, N. Balcon, et al.

(Abstract No155)

Simulation and analysis of spacecraft charging using SPIS-GEO and NASCAP-GEO

Brigitte Theillaumas, Marc Sévoz, Bjarne Andersson, Thomas Nilsson, Jean-Charles Matéo-Vélez, Pierre Sarraih, Benoit Thiébault, Benjamin Jeanty-Ruard, David Rodgers, Nicolas Balcon, Denis Payan

Abstract— **Spacecraft charging issues related to GEO concern all dielectric surfaces susceptible to charge to significant voltages because of the space environment. Testing materials helps defining margins and keeping a good level of confidence on spacecraft resistance to damaging effects. Another aspect of spacecraft charging analysis relies on numerical simulation. Several tools aims at calculating surface charging in harsh environments, in the energy range of some to hundreds of keV, produced by geomagnetic sub storms. Main codes include: NASCAP, SPIS, MUSCAT and Coulomb-2. They use different numerical and sometimes physical models and cross checking their results is a progress need to get better confidence in simulations performed by spacecraft prime manufacturers. The objective of this paper is to simulate different GEO spacecraft configurations with NASCAP and SPIS and to compare the results, both in terms of absolute and differential potentials. The first section corresponds to SCATHA spacecraft. The second part of this paper presents efforts to model a modern telecom spacecraft. Lastly, we conclude on the reliability of the simulations performed and possible rooms for modelling amelioration.**

Keywords—spacecraft charging, numerical simulation, telecom spacecraft, GEO orbit

I. INTRODUCTION

Spacecraft charging effects on equipments can be estimated and studied following several approaches, sometimes coupled. In a first approach, one wants to test the conditions that lead to electrostatic charging and possible electrostatic discharges. This is possibly performed by experimental investigations at system of material levels, as for example in [1]-[2]. A second approach relies on the numerical estimation of the voltages obtained in-flight.

NASCAP (NASA Charging Analyzer Program) is a computer program dedicated to simulate spacecraft charging (dating 1980's). The various formulations are written to levels of accuracy and approximations appropriate to solving problems for geosynchronous environment with short computation duration time. NASCAP capabilities are to define complex objects (3D-cuboidal grid 17x17x33, with cubic elements, narrow cylindrical booms and thin plates), to define materials properties relevant to charging, to calculate electrostatic potentials, to assess shadowing, to calculate primary currents incident on spacecraft surfaces from a plasma/point source, secondary and backscattered electron currents, conductivity, charge accumulation and resulting surface potentials [3]-[4].

The SPIS software (dating mid 2000's) has become today the European standard for the modeling and the simulation of the spacecraft plasma interactions, initially funded on an ESA effort and following an open-source approach in the frame of the SPINE community [5]. Originally designed to focus on scientific applications, the application scope of SPIS is largely wider now and is regularly extended to new engineering applications or domains of physics. This includes, for instance, the modeling of electrical propulsion systems, ESD prediction on solar arrays or link with radiation models through deep charging phenomena. The prediction of the electrostatic charge (absolute and relative) of spacecraft for engineering purposes is also a key issue with modern platforms that are more and more complex. Differential charging can lead to arcing, dangerous for the electronic payload. Absolute charging can induce disturbances on the radio transmission and/or the positioning systems using electric propulsion. This need is especially critical for GEO and MEO missions, where are located most of the commercial platforms. This was the main objective of an ESA funded activity, led by the French SME Artenum which redesigned fully the User Interface, and involving ONERA for solvers enhancement, and OHB-Sweden and Airbus DS for its validation. CNES participated to requirement definition and to validation. The outcome of that European collaboration was the SPIS-GEO tool (improved time simulation and human machine interface ergonomics, suitable for engineering applications).

NASCAP and SPIS results were compared in GEO spacecraft configuration, as well as in a LEO like plasma ground experiment configuration [6]; this latter case being also compared with simulations performed with MUSCAT software [7]. SPIS was also compared with a set of international charging codes [8].

This paper aims at comparing results obtained with SPIS and NASCAP on different configurations. Section II presents a SPIS simulation of the SCATHA spacecraft. Section III relates to a telecom spacecraft in the situation of eclipse exit. Finally Section IV concludes on the main outcomes of this study.

B. Theillaumas and M. Sévoz are with Airbus defence and Space, Toulouse, France (e-mail: brigitte.theillaumas@eads.astrium.net)

J.-C. Matéo-Vélez and P. Sarrailh are with ONERA - The French Aerospace Lab, Toulouse, France (e-mail: mateo@onera.fr)

B. Andersson and T. Nilsson are with OHB sweeden, Sweden (e-mail: bjarne.andersson@ohb-sweden.se

N. Balcon and D. Payan are with CNES (Space Studies National Centre), , Toulouse, France (e-mail: Denis.Payan@cnes.fr

B. Thiébault, Benjamin Jeanty-Ruard are with Artenum , Toulouse, France (e-mail : thiebault@artenum.com)

D. Rodgers is from ESA (European Space Agency), Noordwijk, Netherlands (e-mail: David.Rodgers@esa.int)

(Abstract No155)

II. SCATHA SIMULATION WITH SPIS

The SCATHA (Spacecraft Charging AT High Altitude) satellite was launched in early 1979 as a scientific research satellite by the United States Air Force. On the 24th of April 1979 the spacecraft experienced a severe spacecraft charging event caused by a very extreme plasma environment. The level of spacecraft charge and the local plasma properties were measured by several on-board experiments and is thus scientifically ensured event in-orbit. Today this environment is considered as a worst case scenario for GEO satellites by ECSS.

The main features of the SCATHA satellite include a spacecraft main body, cylindrical in its shape, approximately 1.7 m diameter and length 1.8 m. The top and bottom part of the cylindrical sides were covered in solar panels, and across the middle section there was a so called "belly band" of various experiments and several booms extending. An artistic interpretation of the SCATHA in orbit is presented in Fig. 1. On the top side there were also several experiments located and one omni-directional antenna aligned with the spacecraft's rotational axis. The rotational speed was around one revolution per minute.

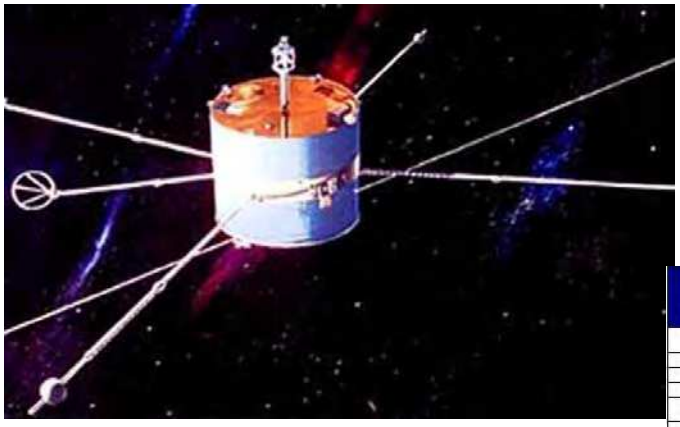

Fig. 1. Artistic view of SCATHA in orbit. (Source: Wikimedia commons, public domain)

Basing the model of SCATHA for the SPIS-GEO simulation on previous model used in the published article by [9], the SCATHA main body is set up as a cylinder with a radius and length of about 0.81 m and length 1.73 m respectively. In order to accurately reproduce published materials the cylindrical sides were divided up into three sections. The bottom part with a height of about 0.69 m corresponded to the lower solar panels. The middle band corresponding to the so called "belly band" with a height of about 0.35 m. This belly band was further divided up into four separate physical surfaces, each segment corresponding to its main surface material. Finally the top part with a height of 0.69 m corresponded to the upper solar panels. The top part was further divided, as it had one experiment segment which was covered with INDOX instead of solar panels.

Extending radially outwards from the middle of the "belly band" there were four booms of radius about 0.04 m and length of about 2.88 m (same as the length used in [9] but in reality they were of varying lengths). The booms were situated in the same fashion, meaning they were separated by 90 degrees with respect to each other, and just as in [9] one of the five experiment booms were not modelled. Neither was the 101.7 m long (tip to tip) electric field antenna extending at the bottom of the SCATHA in Fig. 1 included.

On the top end side of the cylindrical main body a cylindrical boom of radius about 0.04 m extended aligned with the rotational axis, at the end of this boom of length 0.46 m an extra cylinder of radius 0.115 m and length 0.23 m was added. These two cylinders correspond to the omni-directional antenna used in the NASCAP model in [9].

Also on the top side of the cylinder there were several squares and rectangles corresponding to the various experiments modelled in [9] and here given the same surface area and approximate position. Their exact position is not easily replicated using the 3D constructing tool Gmsh. This resulted in a small artificial separation between these surfaces and the edge of the spacecraft cylinder. For the same reason the experiment SC-9 (situated on the top and extended outwards over the edge) was omitted and an artificial separation of 0.03 m was added at the interface between the four radial booms and the cylindrical main spacecraft body.

Any surface materials with a very small value on their resistivity and/or bulk conductivity were considered as conductors. As a rule of thumb any value of NASCAP parameter 13, surface resistivity, less than 10^{14} ohm.m was considered too low. However, as a consequence, this adaptive difference compared with the NASCAP settings will also have some but acceptable effects on the results. Material parameters are presented in Fig. 2, and the geometrical model in Fig. 3.

Node	Surface Material	Spacecraft part	Material properties							
			Material thickness (if dielectric) [m]	Bulk conductivity [mS/m]	Maximum SEEE yield	Energy to produce max SEEE yield [keV]	SEEE yield at 1 keV proton	Energy to produce max SEEE yield [keV]	Photo current density [A/m2]	Surface resistance [Ω*□]
1	Solar Panels	Top and bottom sides of S/C main body	1,79E-04	1 (1E-14)	4,1	0,41	1,36	40	2,00E-05	1 (N/A)
2	INDOX	Patch on the side of S/C main body	1,00E-03	1 (N/A)	1,4	0,8	1,36	40	2,20E-05	1 (N/A)
3	YGOLDC	Booms	1,00E-03	1 (N/A)	1,49	0,48	1	60	2,40E-05	1 (N/A)
4	BOOMAT	Antenna top	5,00E-03	1 (1E-10)	1,86	0,59	0,4	50	2,72E-05	1 (N/A)
5	SCREEN	Experiment (SC5) on top of S/C main body	1,00E-03	1 (N/A)	0	1	0	1	0,00E+00	1 (N/A)
6	GOLD	Experiments on top of S/C main body	1,00E-03	1 (N/A)	0,88	0,8	0,4	50	2,90E-05	1 (N/A)
7	SIO2	Experiment (SC1-3) on top of S/C main body	2,75E-04	2,75E-12	2,4	0,4	1,4	70	2,00E-05	1E16 (N/A)
	BOOMAT		5,00E-03	1 (1E-10)	1,86	0,59	0,4	50	2,72E-05	1 (N/A)
	GOLD		1,00E-03	1 (N/A)	0,88	0,8	0,4	50	2,90E-05	1 (N/A)
	KAPTON		1,25E-04	1E-14	2,1	0,15	1,4	70	2,00E-05	1E15 (N/A)
8	YELLOWC	Part of "Belly band"	5,00E-05	5E-10	2,1	0,15	1,4	70	2,00E-05	1E15 (N/A)
9	BOOMAT	Part of "Belly band"	5,00E-03	1 (1E-10)	1,86	0,59	0,4	50	2,72E-05	1 (N/A)
10	ML12	Part of "Belly band"	1,00E-03	1 (N/A)	1	0,3	1,4	70	2,10E-05	1 (N/A)
0 (SC-ground)	Solar Panels	Solar panels on the side of S/C main body	1,79E-04	1 (1E-14)	4,1	0,41	1,36	40	2,00E-05	1 (N/A)

Fig. 2. Characteristics of the SCATHA SPIS-GEO model

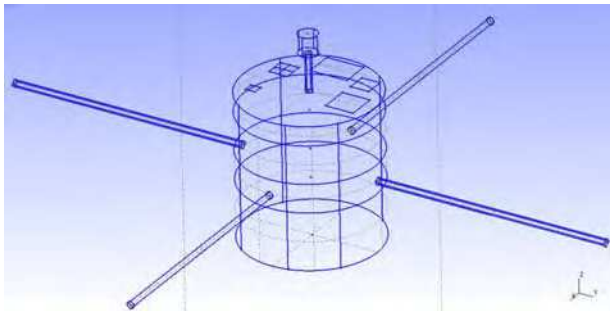

Fig. 3. Model of the SCATHA used in SPIS-GEO for validation and verification simulations

Two plasma environments were used. The first is same as in [9] and presented in Fig. 4. These properties differ from the worst case in ECSS (also based on measurement by SCATHA), but are used in the SCATHA simulations in order to be comparable with the published NASCAP results. The results obtained are consistent with previous NASCAP results. We obtained a spacecraft absolute potential of about -5100 to -5300 V in sunlight configuration, which is comparable to the values reported in [9].

Parameter	Unit	Maxwellian plasma population			
		Electron 1	Ion 1 (H+)	Electron 2	Ion 2 (H+)
Density, n	cm^-3	10	10	10	10
Temperature, T	eV	40 000	20 000	100	100

Fig. 4. Worst case SCATHA environment, dual Maxwellian isotropic plasma

The second environment was specifically simulated with SPIS. It is the ECSS worst case environment in GEO, as measured by SCATHA itself on the 24th of April 1979, in the situation of eclipse, and described in Fig. 5.

	Electrons		Protons	
	Low energy	High energy	Low energy	High energy
Density	0.2 cm^{-3}	1.2 cm^{-3}	0.6 cm^{-3}	1.3 cm^{-3}
Temperature	0.4 keV	27.5 keV	0.2 keV	28 keV

Fig. 5. Plasma populations characteristics

In this case of eclipse in ECSS WC condition, we obtained a spacecraft absolute potential of -7300 V (see Fig. 7). The match with in-flight measurements is satisfactory as the potential fluctuated between -4kV and -8kV during the eclipse in 24 April 1979, see Fig. 6 taken from [10].

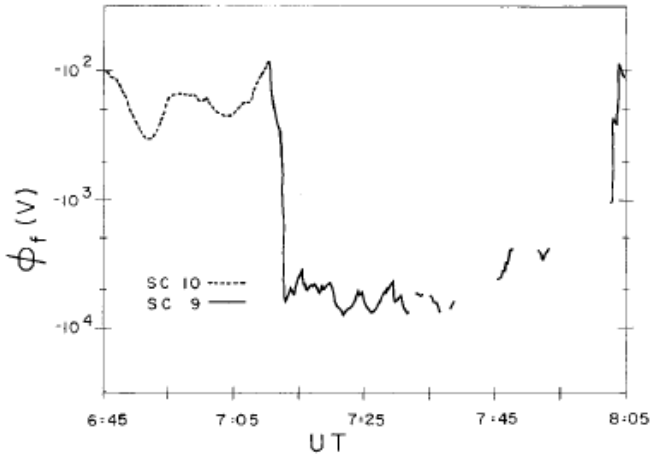

Fig. 6. Frame charging in sunlight (dashed line) and in eclipse (solid line) on 24 April 1979 [10]

3D results are also presented for this eclipse ECSS WC case. The plasma potential in Fig. 7 has the same structure as in [9]. The secondary electron generated under electron and proton impacts have similar profiles, see Fig. 8 and Fig. 9. As a result, they both reduce the spacecraft negative potential. It is worth noticing that a simulation without secondary emission by proton impact led to a spacecraft potential of -23 000 V, which far more negative. Proton impact is of prime importance since the secondary yield can be as large as 1 to 5 for protons of 1 keV to 20 keV. It is combined with the fact that low energy protons are highly focused toward the spacecraft (with a ratio close to the OML factor, i.e. 1-eϕ/kT which can be as large as 50 for 200 eV protons). The positive current due to low energy proton is globally multiplied by a factor of around 100 in comparison to positive current collected by a spacecraft at zero-volt.

Secondary electrons emitted by the negative and quasi-equipotential spacecraft are repulsed by the spacecraft. In particular this explains the "star" shape in Fig. 8 and Fig. 9, which is due to electron deviation by the four booms and by the antenna on top of the spacecraft. Low energy electrons simply follow the electric field lines. The star shape is more pronounced for SEE under proton than under electron impact because a fraction of primary (energetic) electrons are backscattered isotropically with 2/3 of their impacting energy. Those high energetic secondary particles are less influenced by the boom and the global picture is more isotropic.

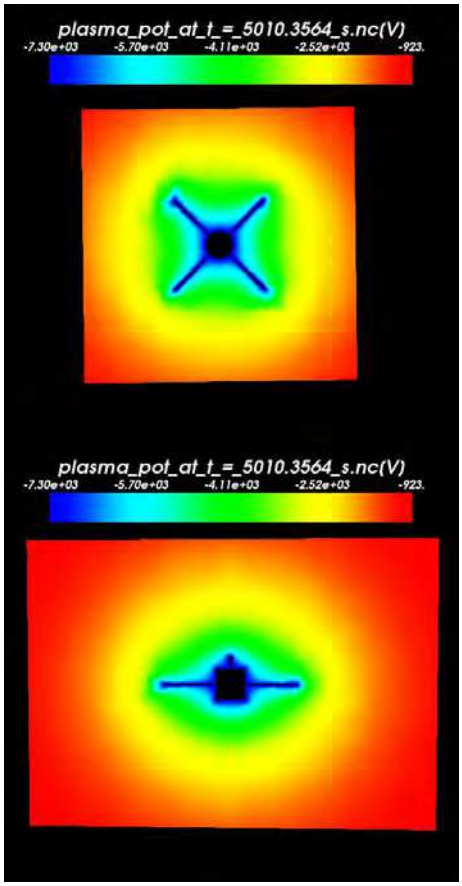

Fig. 7. Worst Potential map around SCATHA in eclipse WC ECSS

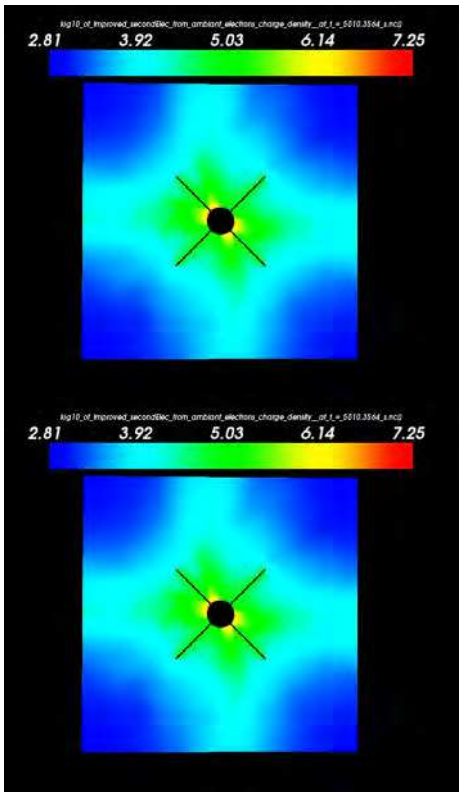

Fig. 8. log10 of density of secondary electron under electron impact in eclipse

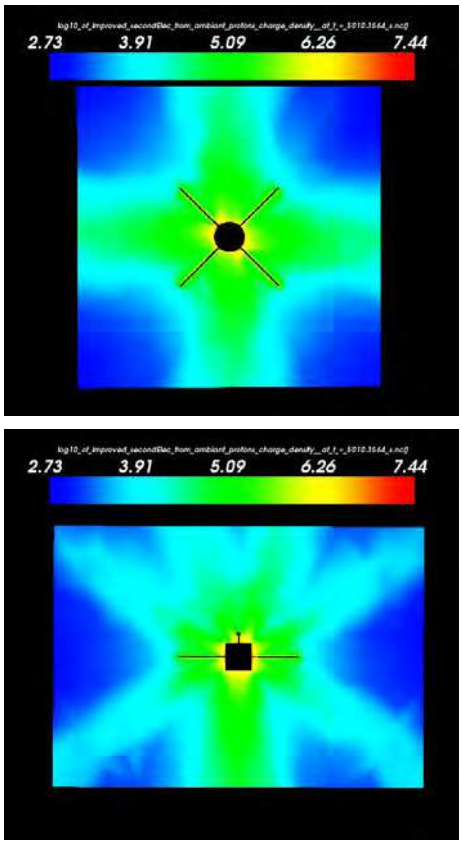

Fig. 9. log10 of density of secondary electron under proton impact in eclipse

III. TELECOM SPACECRAFT COMPARISON

In the frame of R&D initiated with CNES, a telecom spacecraft has been modeled and studied with SPIS-GEO and NASCAP tools.

For SPIS-GEO simulation, the spacecraft consists in a parallelepiped (2.3 x 2.1 x 4 m) and the both solar wings are (2.4m x 18m) spaced with spacecraft with 2.5m length. The top face and side faces (X closures) are covered with MLI (Kapton VDA 25µm) whereas the bottom face is covered with both MLI and Titanium layer (17.5µm). The Titanium layer is used as spacecraft ground for SPIS software. The other sides of the spacecraft (Y walls) are covered with OSR. On solar wing front side, the cover glasses are CMXCOLD (100µm) and transverse/rear sides are modelled with CFRP (125µm).

For NASCAP, based on cubic mesh, all the data are matched with a cubic mesh of 1m length. The spacecraft is (2m x2mx4m). The solar wing is spaced from spacecraft with 2m and solar panels are shorter (2m x 13m) due to the limited grid of the NASCAP-GEO version.

Four antenna reflectors have been modelled. The thermal design is based on two types. The first type is based on CFRP for all faces (rear and active faces) and are implemented on one side of spacecraft, the second type (implemented on the other side of spacecraft) is either white painted with SG121FD paint or covered with a sunshield made of a layer of Kapton coated with Germanium for active face, the both reflectors rear face is covered with standard MLI (Kapton VDA 25µm).

Fig. 10 illustrates the NASCAP materials location on both top and bottom views.

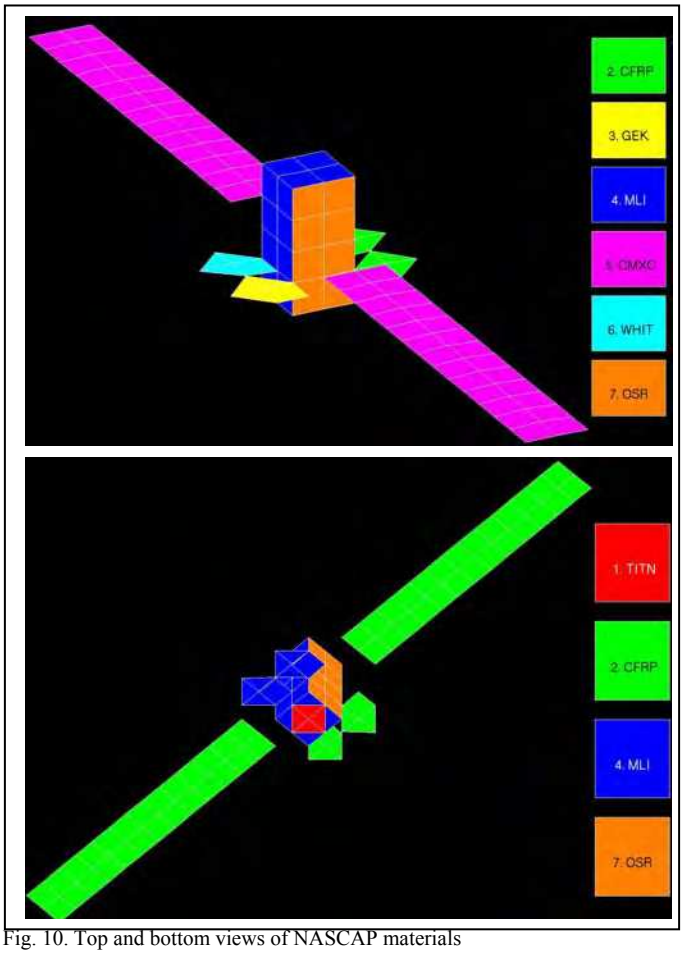

Fig. 10. Top and bottom views of NASCAP materials

Fig. 11 provides the geometry and materials used in the SPIS simulations.

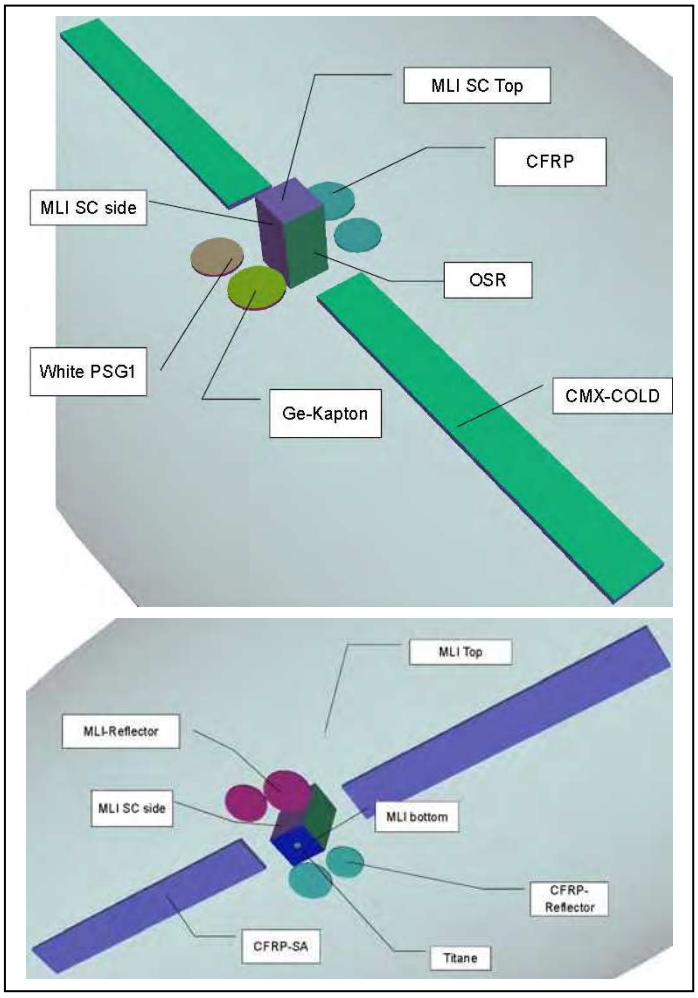

Fig. 11. Top and bottom views of groups editor for SPIS model

The spacecraft configurations are the eclipse one (1000s), the sunlight one (1000s) and the exit from eclipse (2000s). Knowing that NASCAP is not able to deal a time variation of conductivity, which is afforded by SPIS-GEO, the SA cover glasses are assumed to be at cold temperature and have a very high resistivity (1E+16Ω.m), whatever the studied configuration.

The spacecraft is immersed in the ECSS worst-case environment, based on the following worst case isotropic 4π double maxwellian, described in Fig. 12.

	Electrons		Protons	
	Low energy	High energy	Low energy	High energy
Density	0.2 cm^{-3}	1.2 cm^{-3}	0.6 cm^{-3}	1.3 cm^{-3}
Temperature	0.4 keV	27.5 keV	0.2 keV	28 keV

Fig. 12. Plasma populations characteristics

The spacecraft materials properties are identical for both software and are detailed in Fig. 13.

(Abstract No155)

NASCAP n°	Unit	SPIS	TITN	MLI25	OSR_A	CFRP	CMXCOLD	PSG1	GEKAP
1	NA	RDC	1	3.5	4	1	3.5	3.5	1
2	m	DMT	1.70E-05	2.50E-05	1.00E-04	1.25E-04	1.00E-04	7.00E-05	2.50E-05
3	(Ohm.m)-1	BUC	-1	1E-13	4.5E-13	-1	1E-16	-1	-1
4	NA	ATN	22	6	10	6.34	5	5	6
5	NA	MSEY	0.9	2.1	3	0.7	2.2	2.85	1
6	keV	PEE	0.28	0.15	0.21	0.3	0.25	0.25	0.4
7	Angstrom	RPR1	154	80	77.5	110	70	50	80
8	NA	RPN1	0.8	2	0.43	1.9	0.6	0.6	2
9	Angstrom	RPR2	220	400	156	300	150	130	400
10	NA	RPN2	1.76	1.5	1.7	1.04	1.78	1.6	1.5
11	NA	SEY	0.244	0.46	0.244	0.413	0.455	0.244	0.46
12	keV	IPE	230	140	230	135	140	230	140
13	A.m-2	PEY	4.000E-05	2.000E-05	8.000E-05	7.200E-06	2.000E-05	2.000E-05	2.000E-05
14	Ohm.square	SRE	-1	1E+12	1E+15	-1	1E+15	-1	-1
15	V	MAP	10 000	10 000	10 000	10 000	10 000	10 000	10 000
16	V	MPD	11 000	2 000	11 000	11 000	11 000	2 000	2 000
17		RCC	1E-13	2E-12	1E-13	1E-13	1E-13	1E-13	1E-11
18		-	1	1	1	1	1	1	1
19	kg.m-3	MAD	1 000	1 000	1 000	1 000	1 000	1 000	1 000
20		-	20	20	20	20	20	20	20

Fig. 13. Details of material properties

It has to be noted that the Radiation Induced Conductivity (RIC) effect had been excluded during this study.

Fig. 14 illustrates the absolute potentials for the eclipse configuration. The SPIS absolute potential (around -13500V) is more important than for NASCAP (-11300V), which represents a difference of 16% between the two simulations.

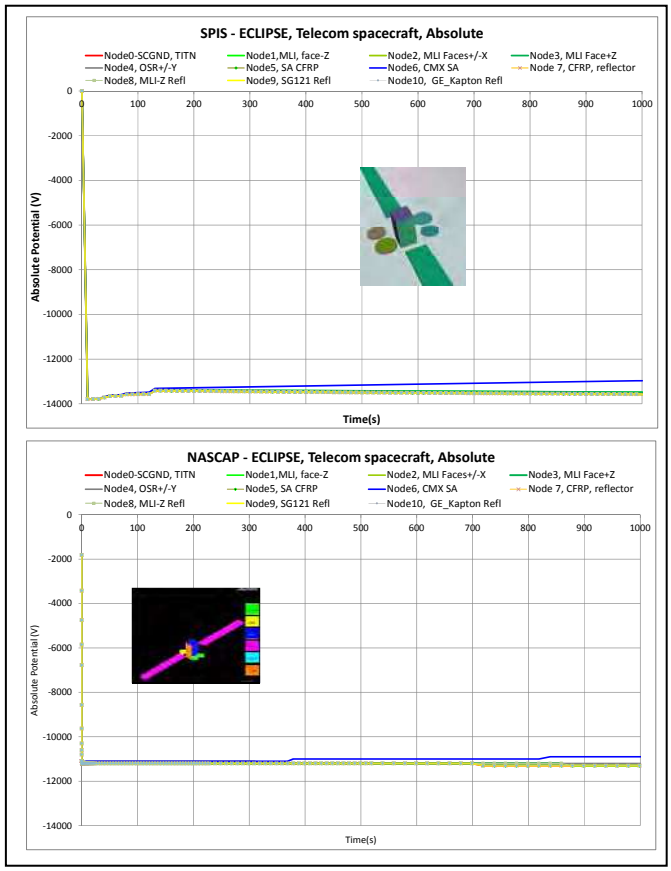

Fig. 14. Absolute potentials for Telecom spacecraft (Eclipse)

Fig. 15 provides the differential potentials profiles based on SPIS and NASCAP simulations. The differential potentials gaps for NASCAP are only due to output format (locked with scientific format 0.00E+00). Due to the fact that the absolute potentials are all above 10000V, the gap is 100V, this explains the step of potentials seen on NASCAP results (that are not physics ones). The cover glasses demonstrate the worst positive differential potential but it has to be noted that NASCAP SA are shorter (13m) than for SPIS case (18m). Cover glasses differential potential (picked at middle of solar wing) is quite lower for NASCAP and may be linked to SA length (NASCAP SA wing is shorter). The NASCAP potential is picked at the middle of solar wing whereas the SPIS cover glasses potential is an average value of both solar wings.

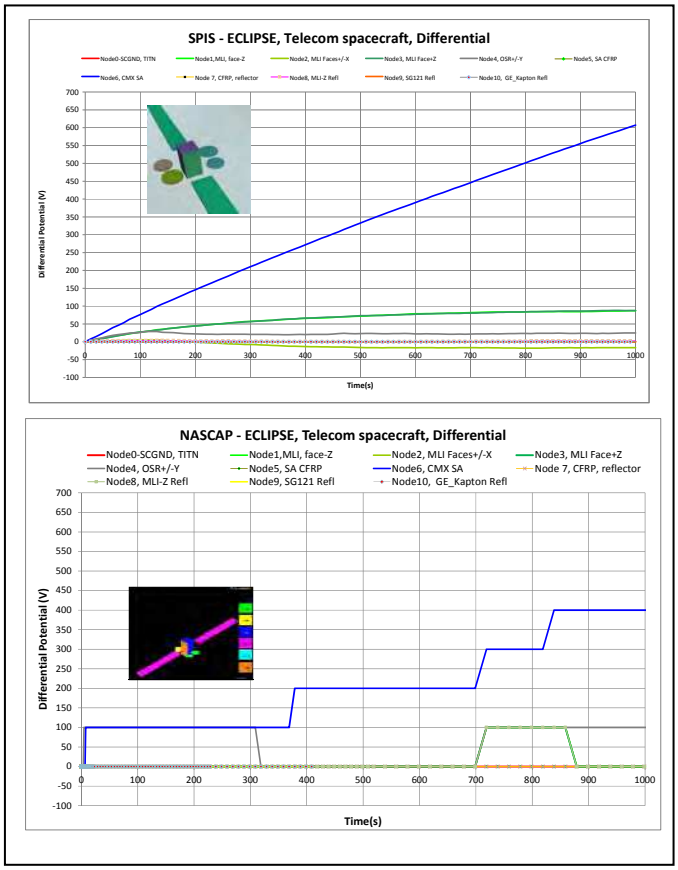

Fig. 15. Differential potentials for Telecom spacecraft (Eclipse)

Fig. 16 provides the differential potentials profile for the spacecraft body dielectric materials (MLIs and OSRs) and provides a good correlation in the 100V range (NASCAP limitation for output data).

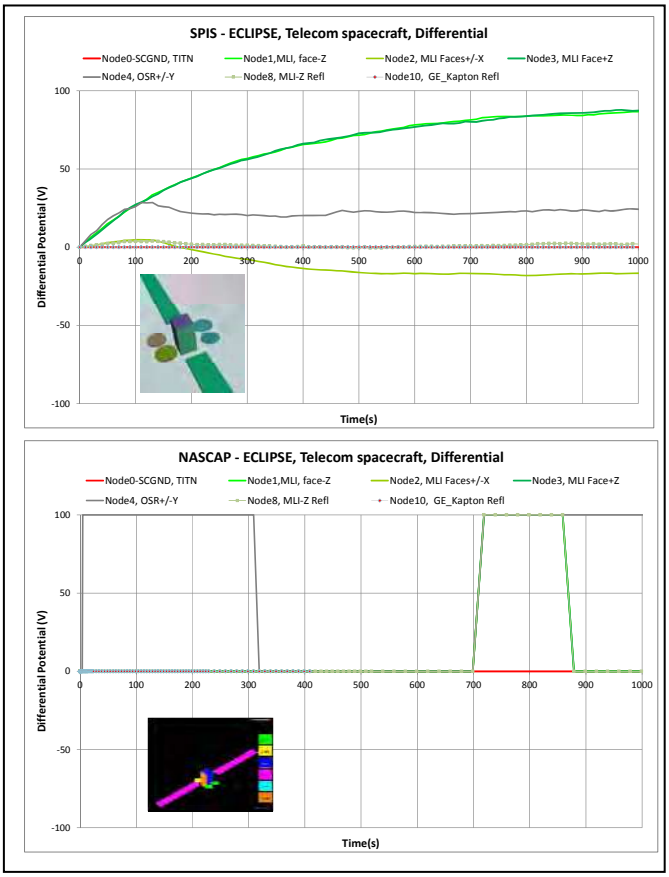

Fig. 16. Differential potentials (Eclipse) for MLIs and OSRs

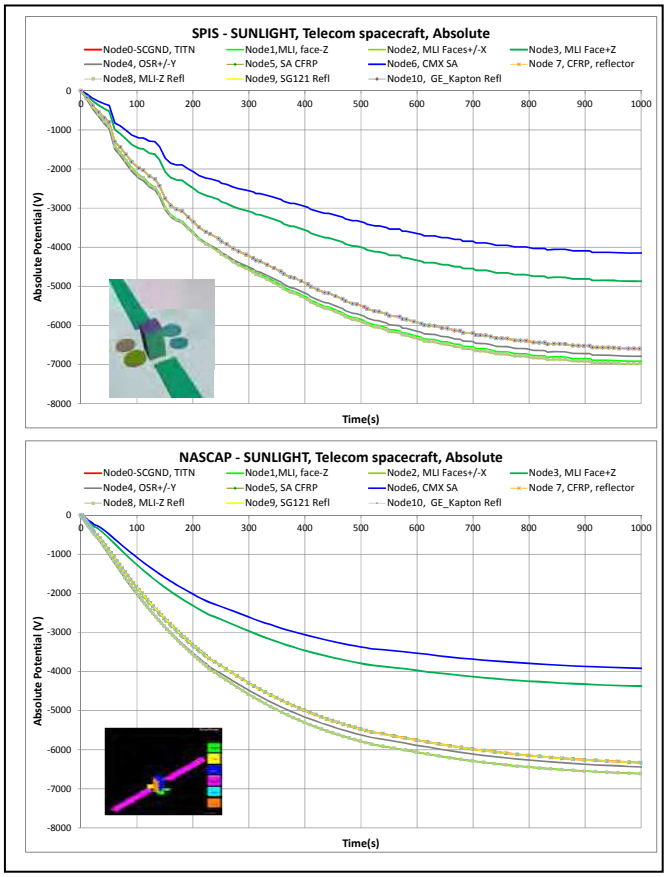

Fig. 17. Absolute potentials for Telecom spacecraft (Sunlight)

The sunlight configuration demonstrates a good correlation between software (-6400V for Titanium for NASCAP, compared to -6600V for SC-GND with SPIS simulation at time equals to 1000 s (a difference of 3%), as shown in Fig. 17.

Fig. 18 illustrates the differential profiles for sunlight configuration (on CMX). The illuminated materials are in IVG (inverted gradient), due to the photo-emission phenomenon. The CMX cover glasses reach a differential potential of +2500V for both SPIS and NASCAP results whereas the MLI on +Z face reaches +1700V for SPIS/ +1900 V for NASCAP.

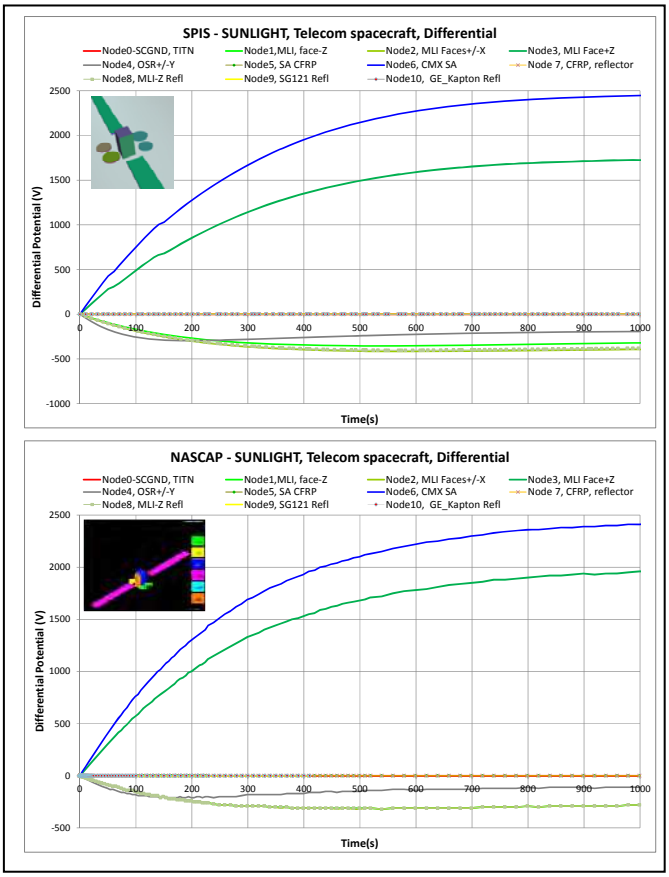

Fig. 18. Differential potentials (Sunlight) for MLIs and OSRs/ All materials

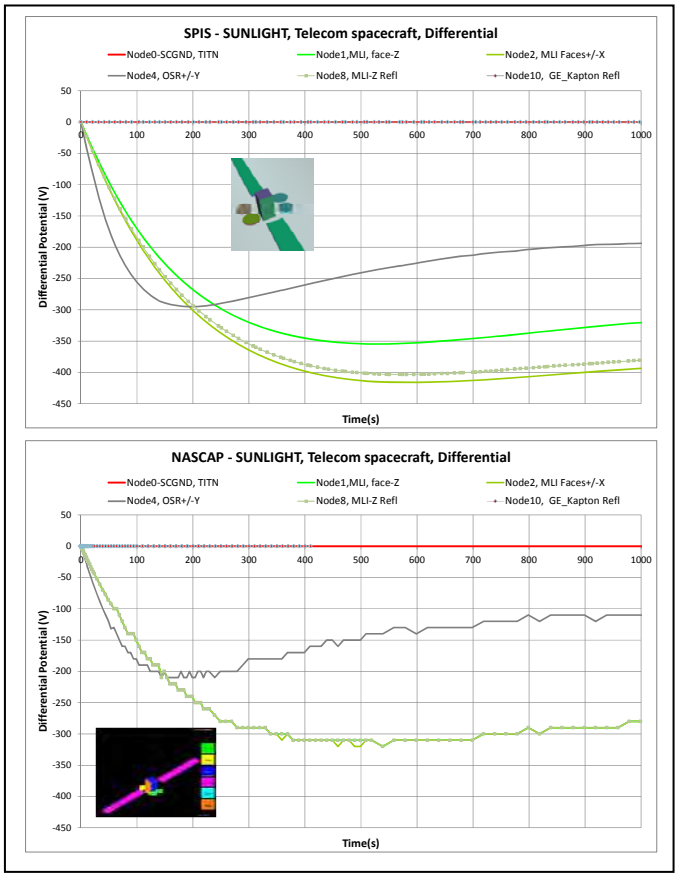

Fig. 19. Differential potentials (Sunlight) for dielectric negative materials

For other materials (no direct illumination, no photo-emission), the differential potentials profiles demonstrate also a good correlation between NASCAP-GEO and SPIS-GEO software as shown in Fig. 19.

For the exit from eclipse (sun intensity raises from “0” to “1” linearly during 60s), phenomena are very similar for both simulations results even if absolute values are different as seen previously for the eclipse configuration.

The profiles of absolute potentials are given in Fig. 20. At the end of eclipse, NASCAP demonstrates -11300V for spacecraft absolute potential, compared to -13500V for SPIS and at the end of run (2000s), NASCAP demonstrates -4600V for spacecraft absolute potential, compared to -6200V. However, one can notice that equilibrium is not fully reached. Moreover the phenomenon of potential barrier blocking the photoemission process for an out of eclipse and the rule that states that the absolute spacecraft potential expected to be in sunlight between third and half the potential achieved during eclipse are also evidenced.

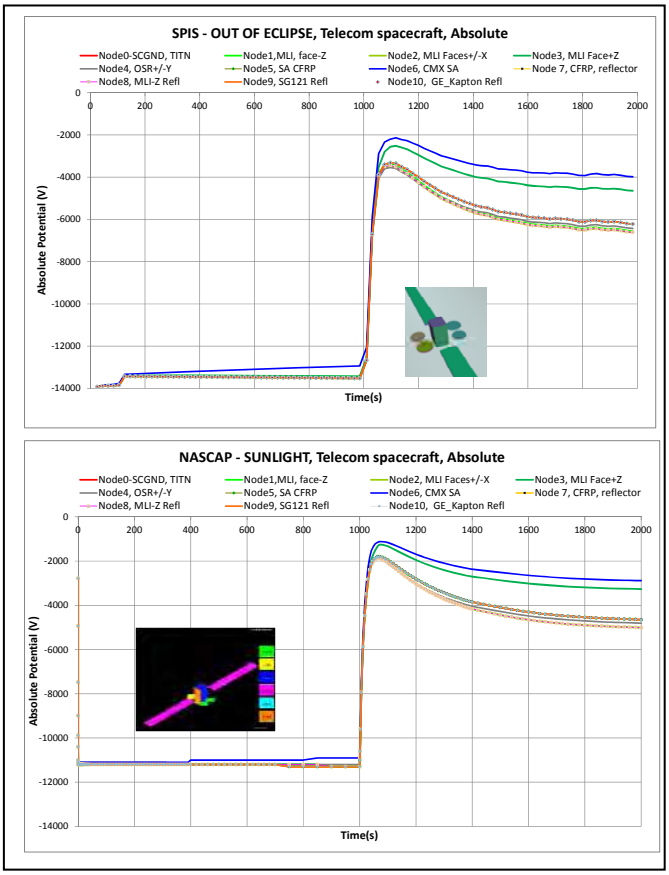

Fig. 20. Absolute potentials for Telecom spacecraft (Out of eclipse)

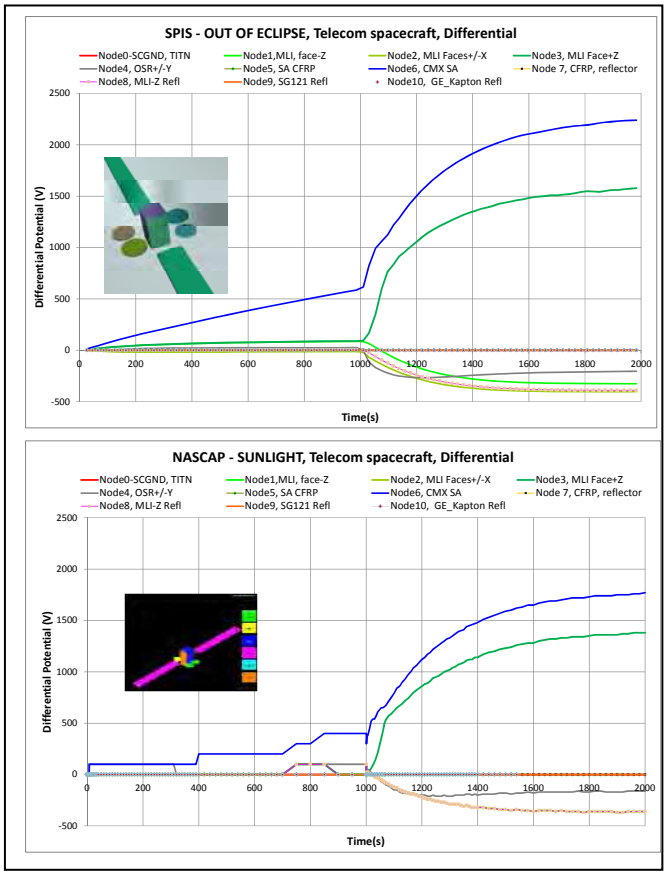

Fig. 21. Differential potentials for Telecom spacecraft (Out of eclipse)

Differential potentials profiles provide satisfactory results, with a relative difference of about 20% as shown in Fig. 21.

When eclipse exit event is finished (60s later) and after, profiles of differential potentials for both illuminated materials (CMX and MLI on top-floor) but also for other dielectric materials (MLI on S/C, MLI on reflectors, OSR) provide a good correlation except for the cover glasses. Cover glasses differential potential is quite lower for NASCAP and may be linked to SA length (NASCAP SA wing is shorter). The NASCAP potential is picked at the middle of SA wing whereas the SPIS potential value is an average value of potentials seen on both wings. As can be seen in Fig. 22, the maximal potential are obtained at the end of the solar array, located far from the spacecraft body.

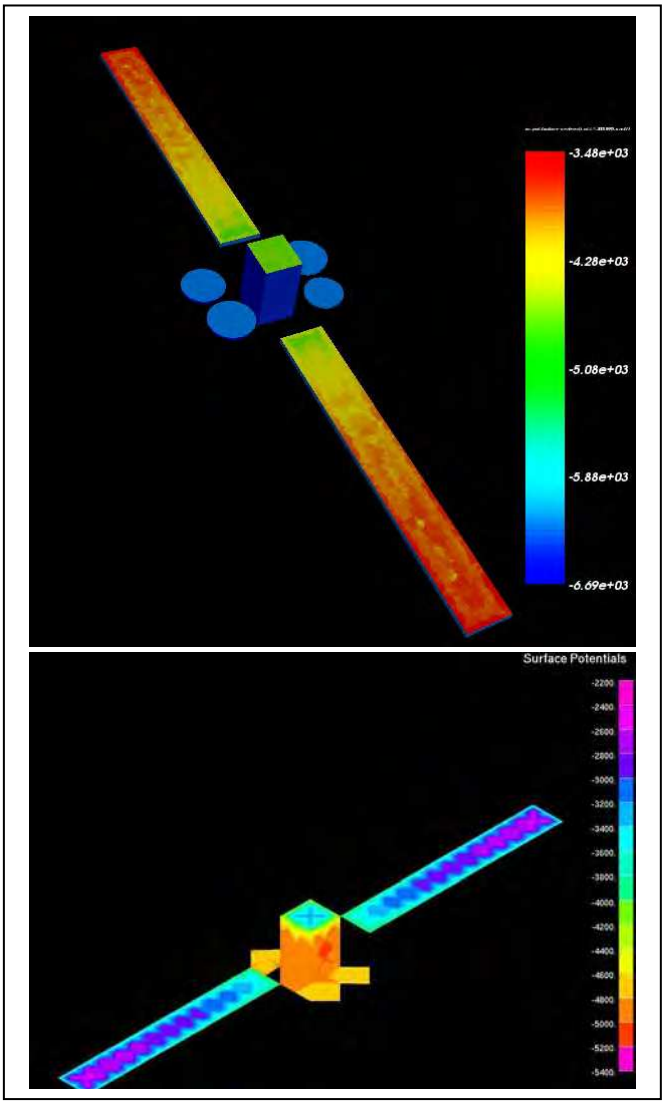

Fig. 22. Solar array potential evolution on solar wings (t= 2000s)

IV. Conclusion

This paper presents significant modelling efforts given to the numerical simulation and comparison of results obtained with two major spacecraft charging analysis tools. In the studied configurations, all in GEO, the results agree qualitatively and also quantitatively. The difference is about 20%, which is deemed satisfactory given the differences in the modelling approaches. The importance of secondary electron emission under electron, photon and proton impact was illustrated, which is not always mentioned for the latter (proton impact). The eclipse exit situation is reproduced and gives perspectives in terms of representativity of the electrostatic discharge risk during that period. Differential charging on cover glasses is enhanced due to still cold materials.

As a first perspective of this work, we suggest to use the SPIS-GEO capability of varying dielectric conductivity as a function of time in eclipse and during eclipse exit. It would add to the precision of the simulation by using results from thermal balance assessment. Another issue concerns the use of material properties as a function of life time, taking into account ageing under space radiations. Finally, the next generation of "all electric" spacecraft offers challenging issues, that could be dealt by using and upgrading SPIS capabilities offered by the ESA AISEPS activity [11].

Acknowledgment

This work was supported partly by ESA in the frame of the SPIS-GEO Contract No. ESTEC/4000101174, and partly by CNES R&D program.

References

[1] T. Okumura, M. Cho, V. Inguimbert, D. Payan, B. Vayner and C.D. Ferguson, 3rd international round-robin tests on solar cell degradation due to electrostatic discharges", J. Spacecraft Rockets, vol. 47, no. 3, pp. 533-541, 2000.

[2] V. Inguimbert, P. Sarrailh, J.-C. Mateo Velez, J.-M. Siguier, C. Baur, B. Boulanger, A. Gerhard, P. Pelissou, D. Payan,, Measurements of the flashover expansion on a real solar panel - preliminary results of emags3 project, IEEE Transactions on Plasma Science, vol. 41, No 12, pp. 3370-3379, 2013

[3] I. Katz et al., A three dimensional dynamic study of electrostatic charging in materials, NASA-CR-135256, 1977

[4] Validation of NASCAP-2k spacecraft environment interactions calculations, V.A. Davis et al., in Proc 8th SCTC, Huntsville, AL, USA, Oct. 2003.

[5] www.spis.org

[6] V.A. Davis, M.J. Mandell, D.C. Cooke, A. Wheelock, J.-C. Mateo Velez, J.-F. Roussel, D. Payan, M. Cho, K. Koga, Comparison of Low Earth Orbit Wake Current Collection Simulations Using Nascap-2k, SPIS, and MUSCAT Computer Codes, Transactions on Plasma Science, vol. 41, No 12, pp. 3303-3309, 2013

[7] T. Muranaka et al., "Final version of multi-utility spacecrat charging analysis tool (MUSCAT)", in Proc 10th SCTC, June 2007.

[8] R. Marchand, Y. Miyake, H. Usui, J. Deca, G. Lapenta, J.C. Mateo-Velez, R.E. Ergun, A. Sturner, V. Genot, A. Hilgers, S. Markidis, Cross-comparison of spacecraft-environment interaction model predictions applied to Solar Probe Plus near perihelion, submitted to Phys. of Plasma.

[9] Schnuelle, G. W., et al, Charging Analysis of the SCATHA satellite, Spacecraft Charging Technology, 1978.

[10] Gussenhoven, M.S. and Mullen, E.G., SCATHA Retrospective: Satellite Frame Charging and Discharging in the Near-Geosynchronous Environment, 6th Spacecraft Charging Technology Conference, AFRL-VS-TR-20001578, 1 Sept 2000

[11] M. Wartelski, C. Theroude, C. Ardura, E. Gengembre, “self consistent simulations of interactions between spacecraft and plumes of electric thrusters”, 33rd international Electric Propulsion Conference, October 2013

Simulation & Analysis of Spacecraft charging with SPIS-GEO & NASCAP

#155 , 13th SCTC Pasadena CA

by ***AIRBUS DS, ONERA, CNES, ARTENUM, ESA, CNES, OHB***

26th of June 2014

Presented by **Marc SEVOZ (AIRBUS Defence & Space)**

AIRBUS DEFENCE & SPACE

Simulations & Analysis of SC charging with SPIS-GEO & NASCAP

BACKGROUND

AIRBUS Defence & Space (former ASTRIUM) used up to now the first NASCAP version (80‘s) for charging simulations

- No possible evolution toward NASCAP-2K
- First scientific SPIS version was complex and large computation times vs. commercial spacecraft needs

!! NEED of updated version => SPIS-GEO tool (ESA study) :

- Artenum redesigned the user interface
- ONERA involved to enhance the solvers
- AIRBUS DS, OHB & CNES involved in the SPIS –GEO software user requirements definition
- AIRBUS DS, OHB & CNES involved in the SPIS –GEO software validation

Further SPIS-GEO / NASCAP comparison is part of the SPIS –GEO tool validation

AIRBUS DEFENCE & SPACE

Simulations & Analysis of SC charging with SPIS-GEO & NASCAP

SCOPE

- Simulate SCATHA charging with SPIS-GEO
- SC potentials vs. different environments (1- one used in published NASCAP results, 2- ECSS specification)
- compare to SCATHA on-flight measurements
- SEEE/SEEP impacts

- Simulate Telecoms SC charging with SPIS-GEO and NASCAP (original version)
- ECSS environment spec
- Compare potentials for Sun, Eclipse, Transition modes

SCATHA simulation

Spacecraft description

- Material properties taken from previous NASCAP simulations [Schnuelle-1978]
- Conductive except some small dielectric patches on top
- 4x 3m length booms

Objectives

- Perform charging analysis using two environments
- Role of secondary electron emission (from electron, proton and photon impacts)

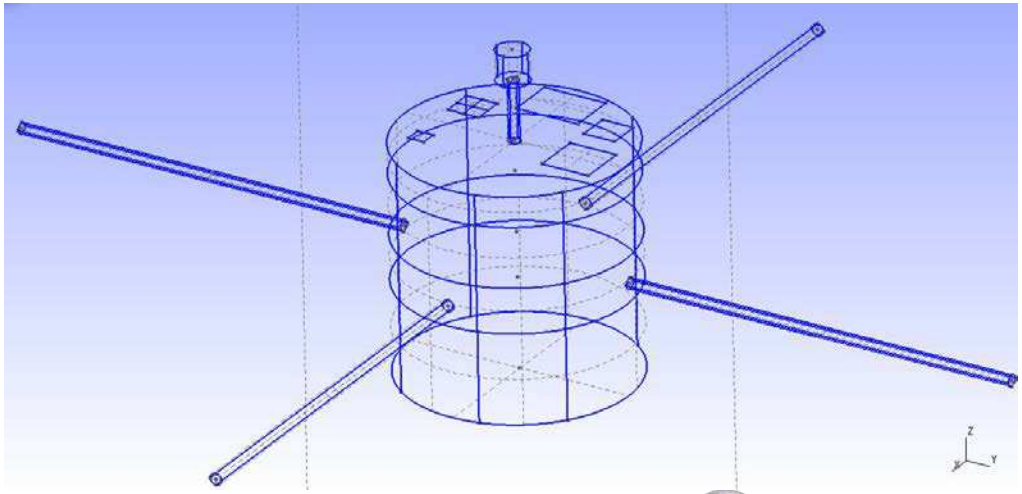

AIRBUS DEFENCE & SPACE

SCATHA vs. Environment 1

Bi-maxwellian plasma @ 1 AU

Parameter	Unit	Maxwellian plasma population			
		Electron 1	Ion 1 (H+)	Electron 2	Ion 2 (H+)
Density, n	cm^-3	10	10	10	10
Temperature, T	eV	40 000	20 000	100	100

Spacecraft absolute potential between -5100 and -5300 V in Sunlight, comparable to -7000V [NASCAP, Schnuelle-1978]

Differences possibly come from

- Detailed SC geometry
- Numerical models
- Secondary electrons emission/recollection (analytical vs PIC)

AIRBUS DEFENCE & SPACE

Scatha vs. Environment 2 - Event of 24 April 1979

Bi-maxwellian plasma
GEO worst case
situation (ECSS spec)

	Electrons		Protons	
	Low energy	High energy	Low energy	High energy
Density	0.2 cm^{-3}	1.2 cm^{-3}	0.6 cm^{-3}	1.3 cm^{-3}
Temperature	0.4 keV	27.5 keV	0.2 keV	28 keV

Spacecraft absolute potential in Eclipse: -7300 V

Consistent with Scatha in-flight measurements during Eclipse in 24 April 1979 (-4 to -8 kV) :

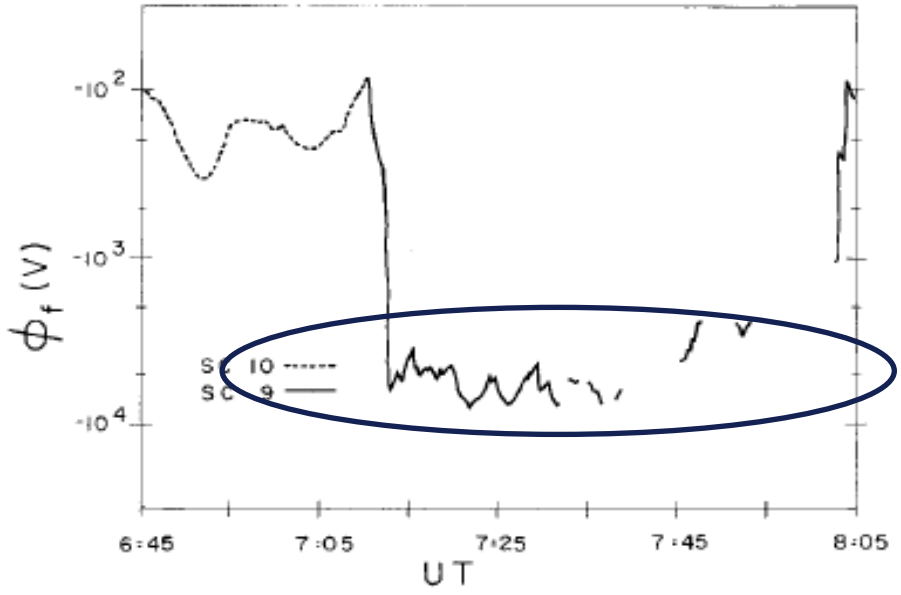

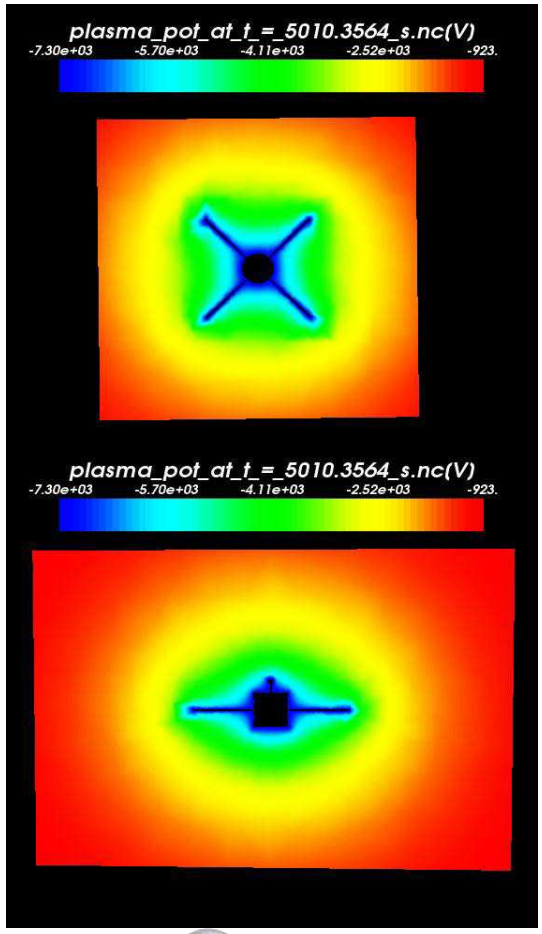

AIRBUS DEFENCE & SPACE

Role of Secondary Electrons

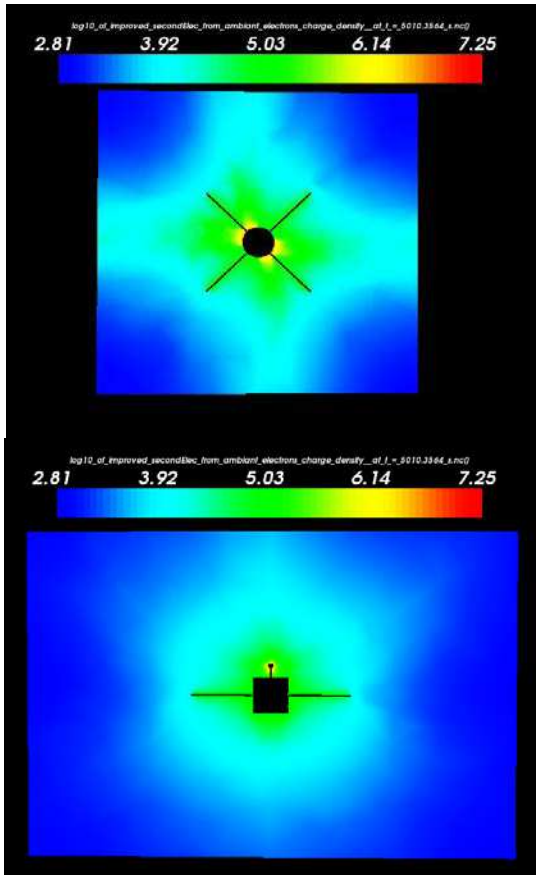

log10 of density of secondary electron under **electron** impact

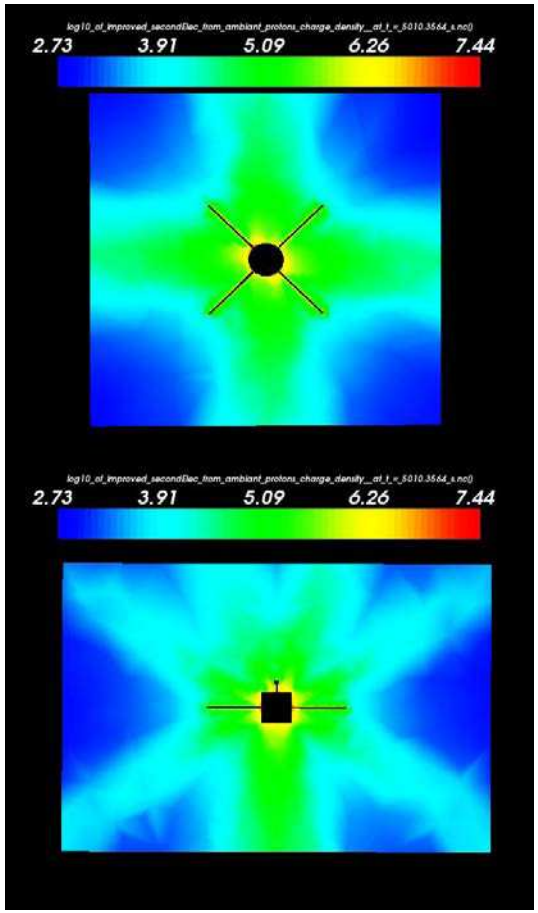

log10 of density of secondary electron under proton impact

Higher density of SEE by protons than SEE by electrons

Importance of low energy protons

- Highly focused to SC (OML factor up to 50)
- Acceleration up to 7keV : Yield for second emission greater than unity (up to 5)

Electrons repulsed by SC follow the electric field lines (booms deviation) : star shape

More pronounced with SEEP since more primary (energetic) electrons backscaterring

Negative spacecraft potential limitation

- **With SEEP -7300 V**
- **Without SEEP -23000 V**

AIRBUS DEFENCE & SPACE

TELECOMS Spacecraft simulation

Spacecraft description

- Platform body dimensions = 2x2x4m
- Surface material properties taken from test data base (heritage)
- Solar wing = 2.4m x 18m (grid limitation = 2x13m in Nascap)
- Deployable antenna reflectors x4
- SC ground = -Z face (titanium layers)

Objectives

- Perform charging analysis with both SPIS-GEO & NASCAP
- Sun, Eclipse (1000s), Transition modes (2000s)
- ECSS GEO environment specification

	Electrons		Protons	
	Low energy	High energy	Low energy	High energy
Density	0.2 cm^{-3}	1.2 cm^{-3}	0.6 cm^{-3}	1.3 cm^{-3}
Temperature	0.4 keV	27.5 keV	0.2 keV	28 keV

AIRBUS DEFENCE & SPACE

TELECOMS Spacecraft simulation

Spacecraft models description

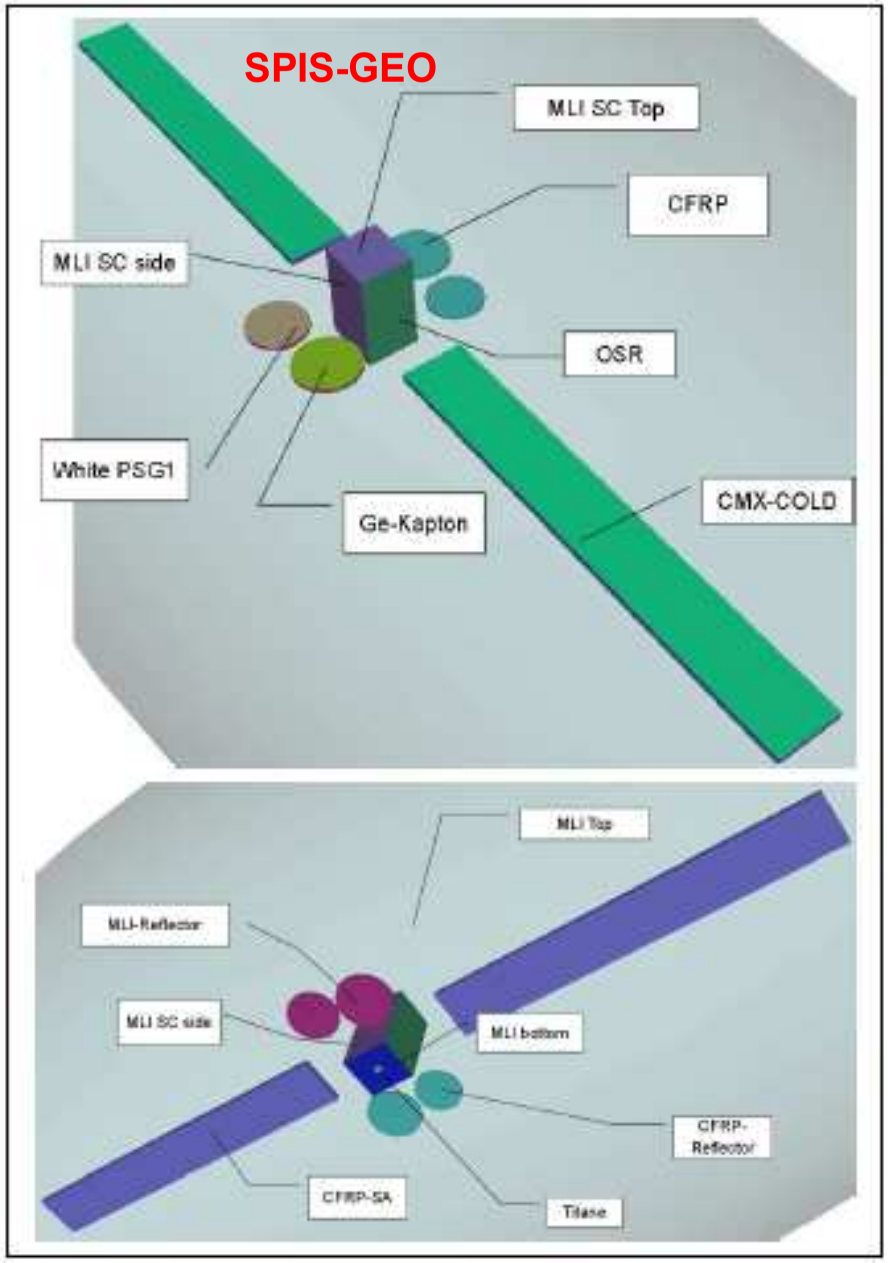

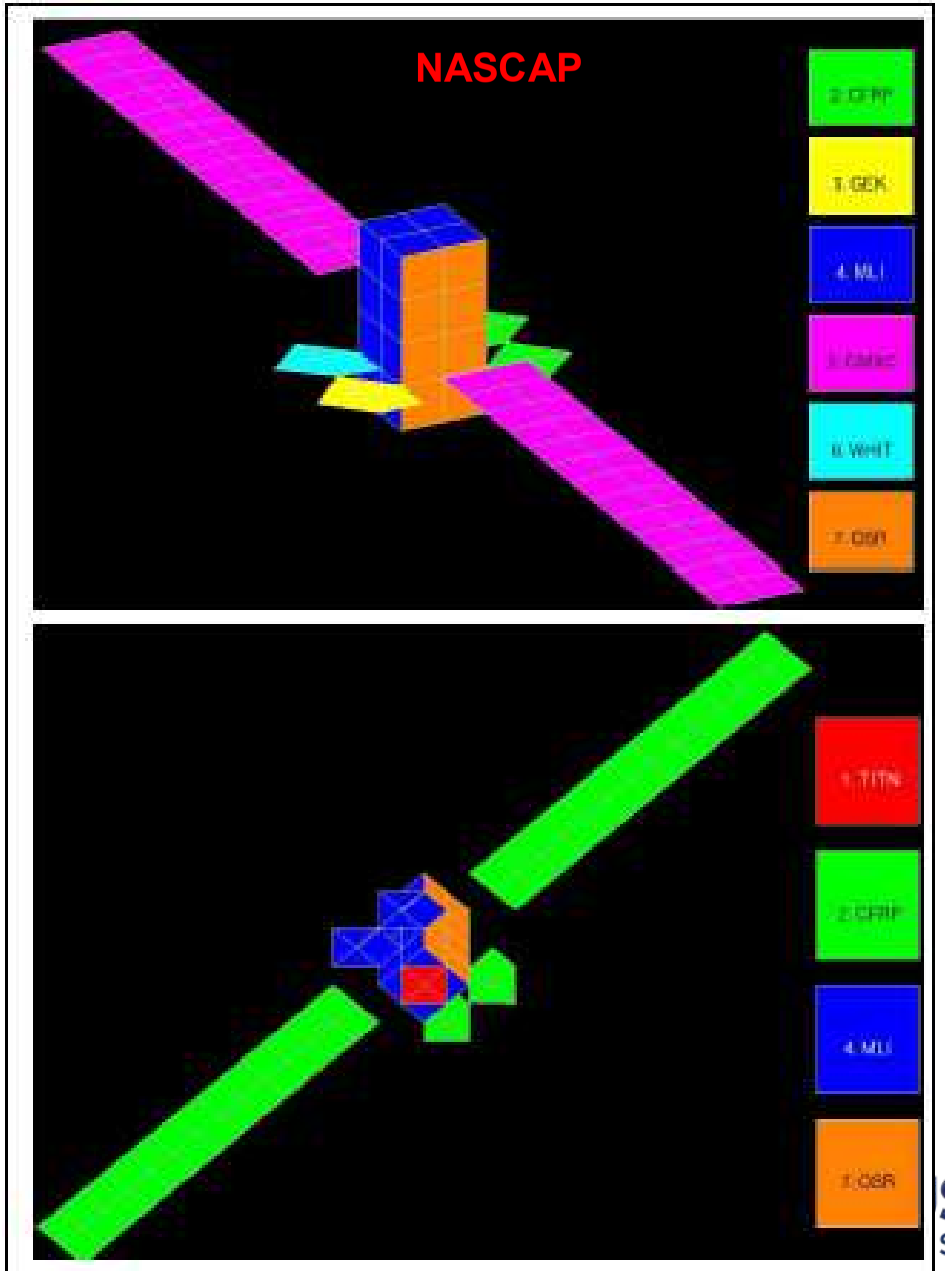

TELECOMS Spacecraft simulation

Absolute/Differential Surface Potentials vs. Time in **ECLIPSE : 20% max difference**

Absolute | **Differential**

SPIS-GEO

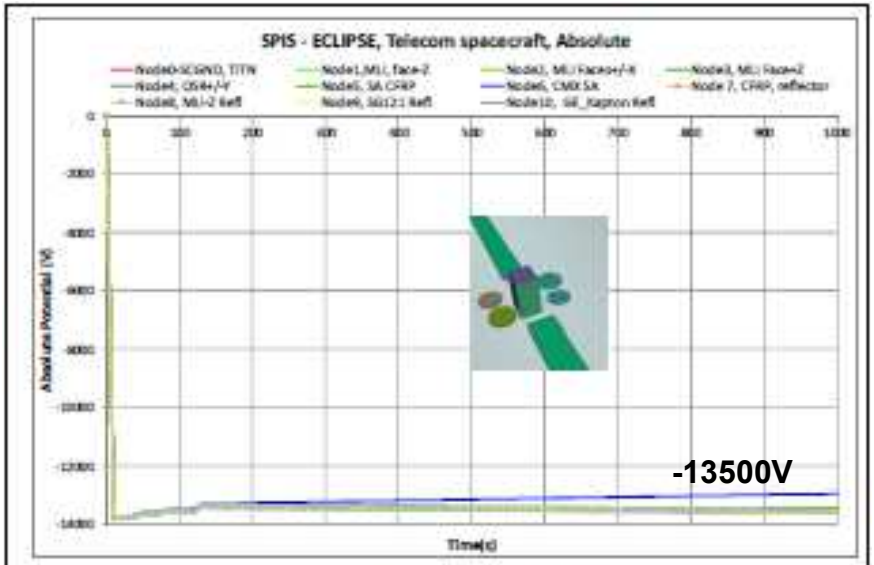

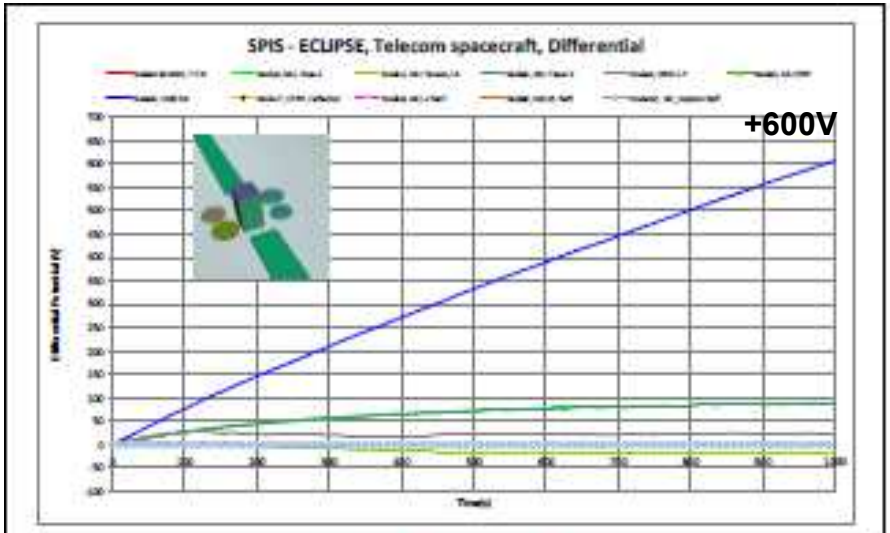

NASCAP

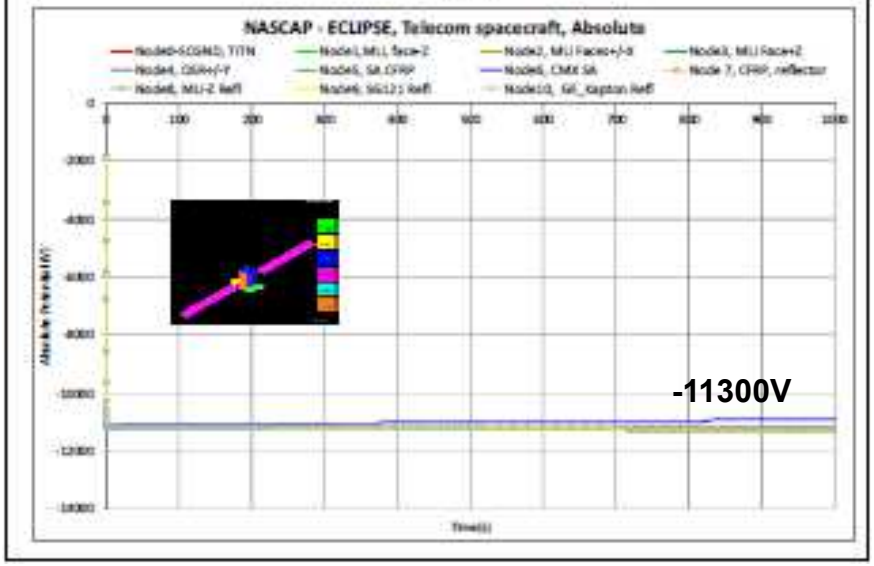

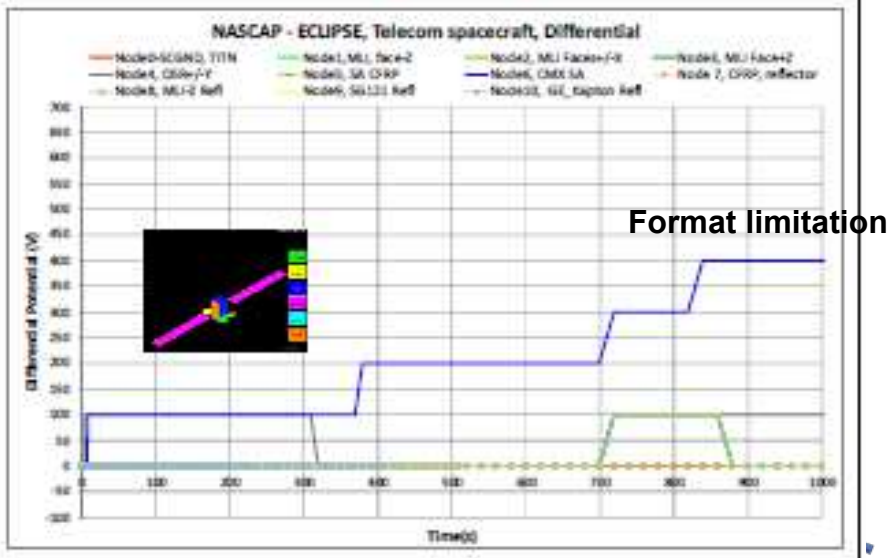

DEFENCE & SPACE

TELECOMS Spacecraft simulation

Absolute/Differential Surface Potentials vs. Time in **SUNLIGHT:** **10% max diff**

Absolute | **Differential**

SPIS-GEO

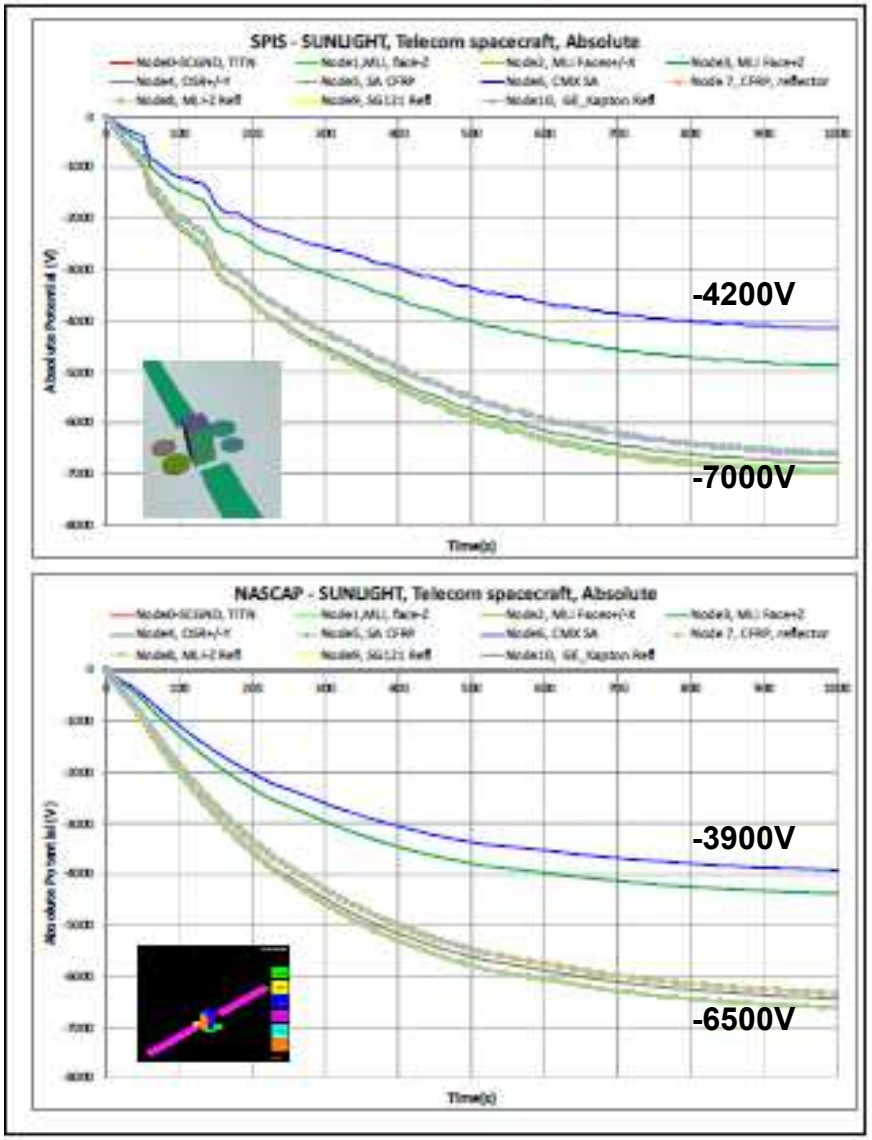

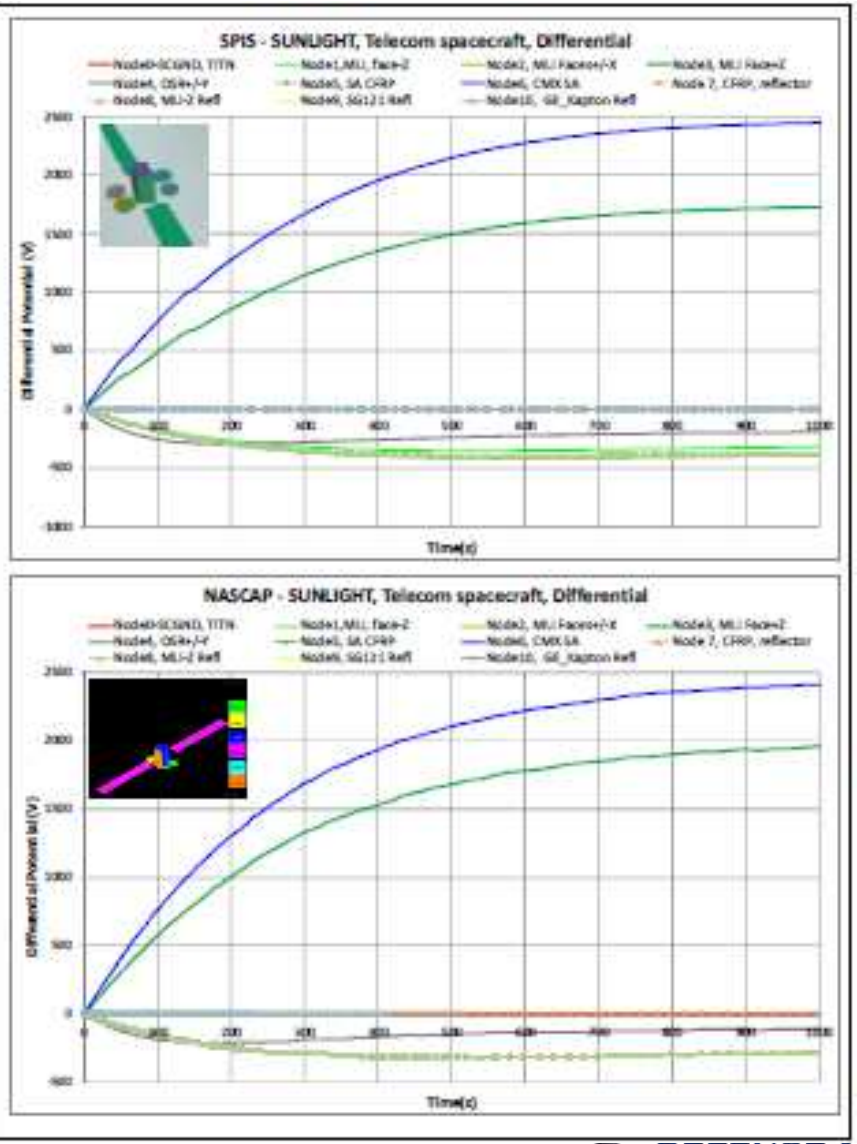

NASCAP

DEFENCE & SPACE

TELECOMS Spacecraft simulation

Absolute/Differential Surface Potentials vs. Time in **ECLIPSE to SUN transition : 20% max diff**

Absolute | **Differential**

SPIS-GEO

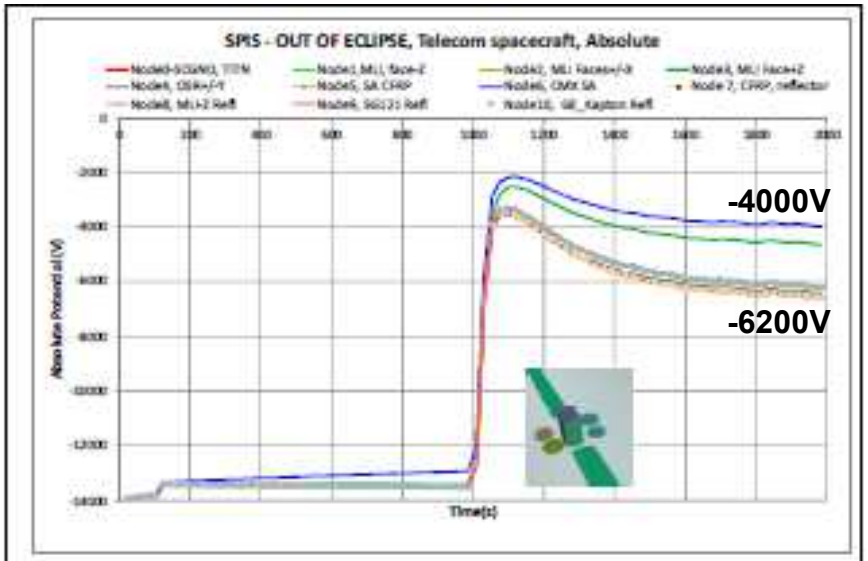

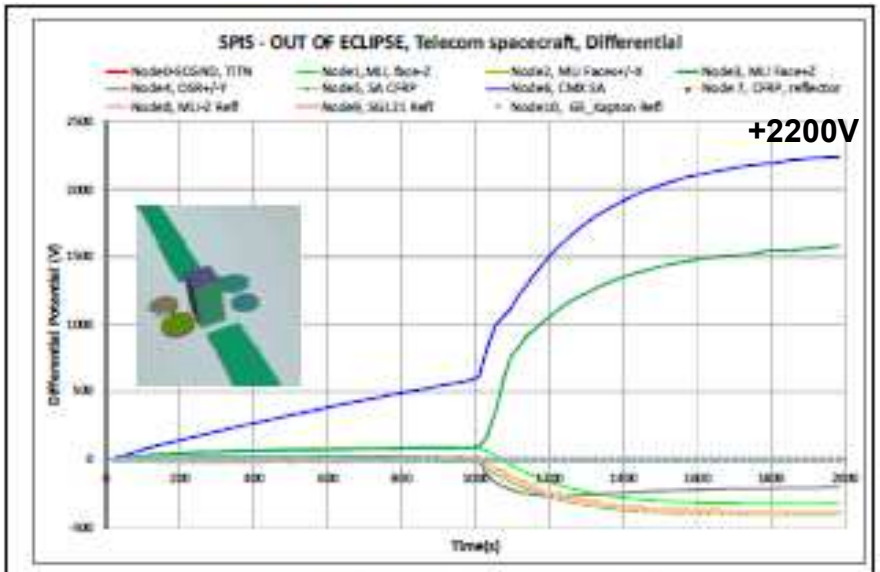

NASCAP

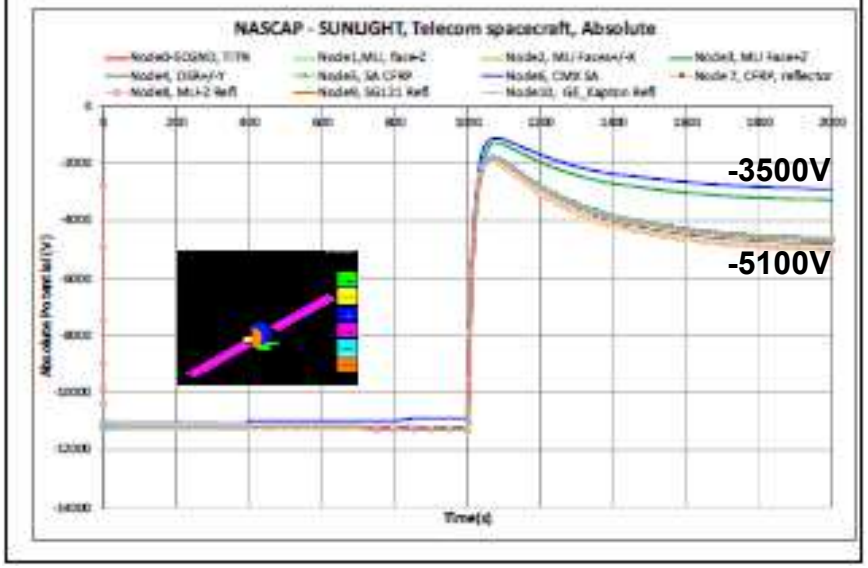

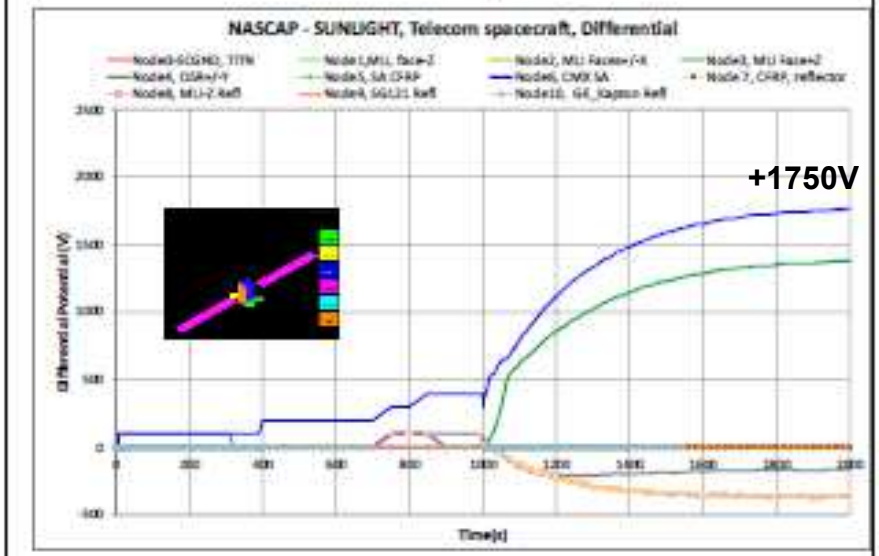

SUMMARY

- Good correlation between SPIS-GEO and Nascap simulations for the 3 main spacecraft configurations (Sun, Eclipse, Transition) : 20% max difference (secondary electrons emission-recollection?)

- Fits (potentials levels and shape) with Scatha on flight measurements

- Major importance of the secondary electrons induced by protons (23kV vs. 7kV)

AIRBUS DS considers SPIS-GEO as fully validated (ergonomy of the user interface, time computation optimization) and suitable for own space Telecoms engineering applications

Outlook

- Electrical propulsion capabilities (ESA AISEPS) exploitation for Electrical Orbit Raising (sputtering, internal charging)

- Elaboration of dedicated SPIS scenario to simulate dynamic variation of the materials conductivities with temperature (ground/flight data), in order to improve accuracy of Eclipse to Sun simulations

Results presented to the next SCTC (stay tuned !)

Thanks to

- Brigitte Theillaumas, AIRBUS DS
- ONERA & Artenum teams for the SPIS-GEO technical support
- CNES & ESA to have initiated and funded this R&D work

Participants :

Brigitte Theillaumas, Marc Sévoz, Bjarne Andersson, Thomas Nilsson, Jean-Charles Matéo-Vélez, Pierre Sarraih, Benoit Thiébault, Benjamin Jeanty-Ruard, David Rodgers, Nicolas Balcon, Denis Payan

Thanks also to my boss who paid the travel to California !

AIRBUS DEFENCE & SPACE

Thank you for your attention !